800 cal./mole higher energy than the *trans* (C_{2h}) form. This difference in energy probably arises largely from steric repulsion between the terminal methyl groups in the skew configuration. In the skew configuration of 2-thiabutane, by virtue of the C–S bond distance being longer than the C–C bond distance, the terminal methyl groups are farther apart than in the skew configuration of *n*-butane. This greater separation of the methyl groups must reduce the steric repulsion between them to the point where it does not result in any energy difference between the rotational isomers large enough to detect by current spectroscopic or thermodynamic methods.

Summary

The heat capacity of 2-thiabutane in the solid and liquid states was measured over the temperature range 14–298°K. The melting point (167.23 ± 0.05°K.) and heat of fusion (2,333 cal./mole) were determined. The vapor pressure was measured over the temperature range 23–101° and the following equation was selected to represent the data: $\log_{10}p = 6.93849 - 1182.562/(t + 224.784)$. The heat of vaporization was measured at 301.66, 319.76 and 339.81°K., and the values found were 7563, 7329 and 7055 cal./mole, respectively. The heat capacity of the vapor was measured at five different temperatures in the range 327 to 487°K. The experimental values of $C_p{}^0$, the heat capacity of the ideal gas state, may be represented by the equation: $C_p{}^0 = 5.11 + 6.5448 \times 10^{-2}\,T - 2.1735 \times 10^{-5}\,T^2$. An equation for the second virial coefficient, B, in the equation of state $PV = RT + BP$ was obtained from thermal data. This equation is B (cc.) $= -257 - 68.13 \exp(900/T)$. The entropy of liquid 2-thiabutane at 298.16°K. is 57.14 ± 0.10 cal./deg./mole, and the entropy of the vapor in the ideal gas state at the normal boiling point, 339.81°K., is 82.70 ± 0.15 cal./deg./mole.

A vibrational assignment was made for 2-thiabutane. Interpretation of the spectroscopic data led to the conclusion, which was confirmed by the thermal data, that the two rotational isomers have nearly the same energy. The heights of the potential barriers hindering internal rotation which were selected to fit the calorimetric data are 1970 cal./mole for rotation about either C–S bond and 3820 cal./mole for rotation about the C–C bond. The thermodynamic functions $(H^0_0 - F^0_T)/T$, $H^0_T - H^0_0$, S^0 and $C_p{}^0$ were computed for selected temperatures up to 1000°K.

BARTLESVILLE, OKLAHOMA RECEIVED JULY 20, 1950

[CONTRIBUTION FROM THE RESEARCH LABORATORY OF THE GENERAL ELECTRIC COMPANY]

Empirical Analysis of Viscosity Data[1]

BY H. TRACY HALL AND RAYMOND M. FUOSS[2]

Introduction

The capillary viscometer is essentially a device in which a volume V of liquid flows through a capillary of length l and radius R in t seconds under a pressure of p g./cm.^{2}. Using Poiseuille's equation, we may calculate the viscosity η (in poises) by the relationship

$$\eta = \pi g p R^4 t/8Vl \qquad (1)$$

For a given viscometer, the product pt should be constant if (1) is satisfied; actually, as is well known, the product usually increases as the driving pressure decreases. Three effects, inherent in the design of the viscometer, contribute to this variation: (1) all of the work done by the driving pressure is not dissipated as heat in overcoming viscous friction; (2) flow near the ends of the capillary is not laminar; (3) the volume of liquid which flows from the bulb is not the volume of the dry bulb. Of these, the first is usually the largest correction term for ordinary liquids ($\eta \approx 10^{-2}$) in conventional viscometers. If correction is made for these instrument effects, and the pt product still varies with driving pressure, then we may conclude that the liquid is non-Newtonian, *i.e.*, that $\eta = \eta(p)$. For the usual range of driving pressures (giving average velocity gradients of the order of 10^3 seconds^{-1}), $1/pt$ is linear in p over a much wider range of variables than that corresponding to linearity of pt in $1/t$. We present in this paper an empirical analysis of viscosity data, which permits isolation of the shear-dependent term of the viscosity.

Kinetic Energy and End Effect Corrections.—The liquid leaving the viscometer capillary is travelling with finite velocity; therefore, only part of the work done by the driving pressure overcomes viscous friction within the capillary. The corresponding correction has been accordingly called the kinetic energy correction. Wilberforce[3] made an important correction to Hagenbach's[4] first estimate of this quantity and also made an estimate of the end effects on Reynolds'[5] analysis of the transition from laminar to turbulent flow. Wilberforce's result may be written

$$\eta = \pi g p R^4 t/8Vl - m\rho V/8\pi l t \qquad (2)$$
$$= \alpha p t - \beta/t \qquad (2')$$

If the constant m were unity, the second term on the right then would be the kinetic energy correction, calculated on the assumption that the flow throughout the length of the capillary were laminar; *i.e.*, $m = 1$ corresponds to the case of negligible end effects. Ample experimental evidence shows that, while m is near unity, its actual value is somewhat greater. In other words, practical viscometers have end effects which may not be neglected. A

---

[1] Presented at the Schenectady Meeting of the National Academy of Sciences, October, 1950.

[2] Yale University, New Haven, Conn.

[3] L. R. Wilberforce, *Phil. Mag.*, **31**, 407 (1891); *cf.* also G. Barr "Monograph on Viscometry," Oxford University Press, London, 1931, p. 16.

[4] E. Hagenbach, *Pogg. Ann.*, **109**, 385 (1860).

[5] O. Reynolds, *Phil. Trans.*, **174**, 935 (1883).

precise calculation of m (or its equivalent) would involve the integration of the Navier–Stokes equation with almost hopelessly complicated boundary conditions. It seems preferable, therefore, to accept (2) as the summary of much experimental evidence and to proceed from this equation as our starting point.

We may consider Equation (2) as a quadratic in $(1/t)$ with the solution

$$1/t = (\eta/2\beta)[(1 + 4\alpha\beta p/\eta^2)^{1/2} - 1] \qquad (3)$$

The variable in the radical is to a close approximation $m\rho V/2\pi l\eta t$, which is about $6/t$ for $m \approx 1$, $\rho \approx 1$, $V = 4$, $l = 10$, $\eta \approx 0.01$. For ordinary work, therefore, we may expand the radical and drop cubic and higher terms; to this approximation

$$1/t = \alpha p/\eta - \alpha^2\beta p^2/\eta^3 \qquad (3')$$

which immediately leads to the alternative form of (2)

$$\begin{aligned} 1/pt &= (\pi g R^4/8Vl\eta) - (\pi g^2 R^8 m\rho p/8^3 V l^3 \eta^3) && (4)\\ &= \mathrm{I} - Sp = A/\eta - A'\rho p/\eta^3 && (4') \end{aligned}$$

Equation (4) states that a Newtonian liquid in a viscometer which needs correction for kinetic energy and end effects will give pt reciprocals linear in the driving pressure; *i.e.*, apparent fluidity is linear in p, and the true value of $1/\eta$ is obtained by extrapolating $(1/pt)$ to zero pressure and dividing by the instrument constant A. This in turn is evaluated by calibration with liquids of known viscosity. Water[6] is usually taken as the standard, with $\eta = 0.008929$ at 25.00°.

Drainage Correction.—Equation (4) was derived on the tacit assumption that V was equal to V_0, the volume of the dry bulb. This value is correct, if we run into a dry bulb, as recommended by Swindells[6]; if a filled bulb is being drained, however, allowance must be made for the liquid which remains in the bulb, wetting the walls.[7] We expect the volume of this liquid to be given by

$$\Delta V = a\eta/\rho t \qquad (5)$$

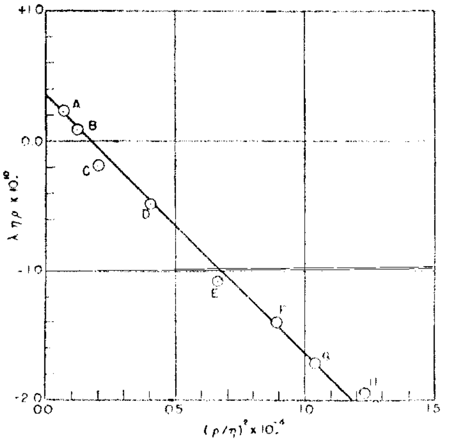

Fig. 1.—Test of Eq. (8): (A) 36.6% of sucrose in water, (B) 32.2% sucrose, (C) 27.7% sucrose, (D) 19.6% sucrose, (E) 91.6 wt. % nitrobenzene in methanol, (F) 80.7 wt. % nitrobenzene in methanol, (G) 72.8 wt. % nitrobenzene in methanol, (H) water.

where a is an empirical constant depending on the geometry of the viscometer bulb. (It may also depend on surface tension of the liquid, but we have insufficient evidence at present to decide this point.) Correcting (1) for ΔV, we see that the coefficient A of (4′) becomes

$$A = k/V = k/(V_0 - \Delta V) \qquad (6)$$

where V is the volume of liquid which actually passes through the capillary in t sec. Substituting (6) in (4′) and dropping higher terms, we obtain

$$\begin{aligned} 1/pt &= A/\eta - (A'\rho/\eta^3 - aA^2/\rho V_0\eta)p && (7)\\ &= A/\eta - \lambda p && (7') \end{aligned}$$

where A now means $\pi g R^4/8V_0 l$.

Comparison with Experiment.—It will be seen that the slope of the $(1/pt)$—p plot is made up of two terms of opposite sign, each of which depends explicitly on the viscosity of the test liquid. For liquids of increasing viscosity, therefore, we would expect a reversal of the sign of the slope at high viscosities, when the drainage correction exceeds the Wilberforce correction. This has been observed experimentally, for a series of sucrose–water and nitrobenzene–methanol mixtures, by W. N. Maclay of Yale University, who has kindly made his data available to us. The most direct test of Equation (7) is obtained as follows: we multiply the coefficient λ by $\eta\rho$ and obtain

$$-\lambda\eta\rho = aA^2V_0 - A'(\rho/\eta)^2 \qquad (8)$$

In Fig. 1, we show a plot of Maclay's slopes (multiplied by $\eta\rho$) as a function of $(\rho/\eta)^2$. It will be seen that the points average to a straight line as required by Equation (8). From the intercept at $(\rho/\eta)^2 = 0$, we obtain the drainage correction, and from the slope, the Wilberforce coefficient may be evaluated.

It will be noted that a knowledge of the viscosity was necessary in order to carry out the test shown in Fig. 1. Having used these data to determine the (small) drainage correction, we may now test Equation (4) in a completely empirical fashion. In the form (4′), Equation (4) states that the $(1/pt)$–p plot is linear with intercept I at $p = 0$ and with slope S (assuming no drainage). We may use the result of the extrapolation in Fig. 1 to correct the observed slopes to give values of S

$$S = \lambda + aA^2V_0/\eta\rho \qquad (9)$$

The viscosity is readily eliminated between I and S giving

$$I = A(S/A'\rho)^{1/3} \qquad (10)$$

A plot of log I against log S/ρ is shown in Fig. 2 for a variety of systems; the straight line was drawn with a slope of one-third. It will be seen that the points conform closely to the result expected from Equation (10).

Using the Wilberforce values of I and S, as given in Equation (4) to eliminate R, we obtain the equation

$$\rho/\eta = (8\pi l/mV_0)(S/I^2) \qquad (11)$$

In Fig. 3, ρ/η is plotted against S/I^2. The points may be averaged by a straight line through the origin, from which we obtain $m = 1.15$ for $l = 11.0$ cm. and $V_0 = 4.02$ cc. It should perhaps be mentioned that the scattering of the points in

---

[6] J. F. Swindells, *J. Colloid Sci.*, **2**, 183 (1947).

[7] G. Jones and R. E. Stauffer, This Journal, **59**, 1630 (1937); R. M. Fuoss and G. I. Cathers, *J. Polymer Sci.*, **4**, 97 (1949).

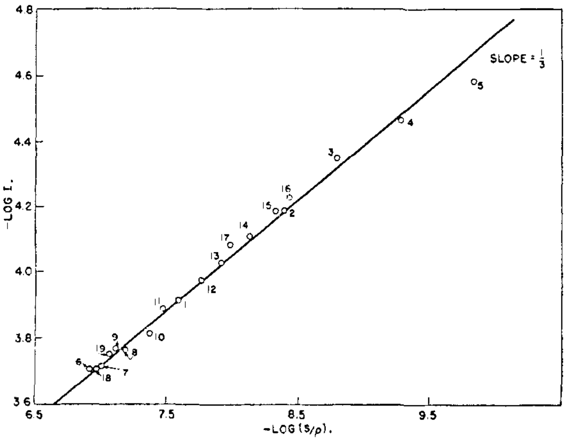

Fig. 2.—Plot of log I *vs.* log S/ρ for various liquids: 1, H_2O; 2, 19.6% sucrose; 3, 27.7% sucrose; 4, 32.3% sucrose; 5, 36.6% sucrose; 6, MeOH; 7, 5.4% $PhNO_2$ in MeOH; 8, 22.5% $PhNO_2$ in MeOH; 9, 24.5% $PhNO_2$ in MeOH; 10, 38.6% $PhNO_2$ in MeOH; 11, 55.6% $PhNO_2$ in MeOH; 12, 72.8% $PhNO_2$ in MeOH; 13, 80.7% $PhNO_2$ in MeOH; 14, 91.6% $PhNO_2$ in MeOH; 15, 98.0% $PhNO_2$ in MeOH; 16, $PhNO_2$; 17, EtOH; 18, PhMe; 19, $MeNO_2$.

Fig. 3 is within the experimental error of determining a *slope*, where the *total* change in apparent viscosity over our pressure range was of the order of only one per cent.

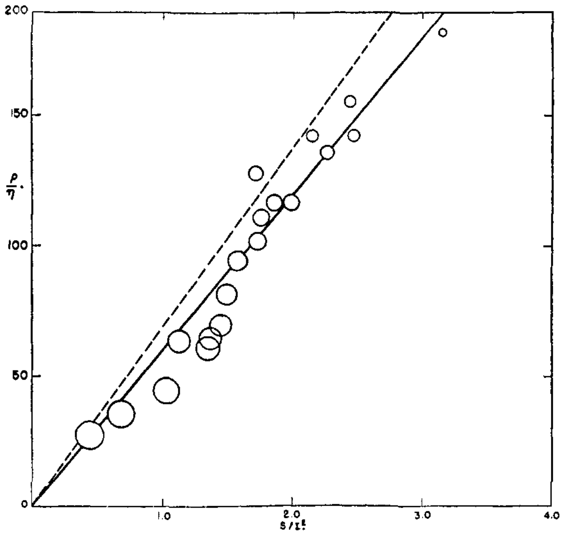

Fig. 3.—Test of Equation (11): dotted line, $m = 1$.

Structural Viscosity.—Solutions of polymers, especially at higher concentrations or at high molecular weights, or when the polymer carries an electrostatic charge, usually show a dependence of apparent viscosity on the rate of shear.[8,9] Extrapolation to zero rate of shear on the Bingham plot is generally impossible, because the pt–$(1/t)$ plots are frequently curved. However $(1/pt)$–p curves for several systems investigated are linear. We are indebted to R. A. Mock of the Sterling Chemistry Laboratory of Yale University for the data of Fig. 4, which gives the $(1/pt)$–p plots for a series of solutions of polyvinylpyridine in methanol. The polymer has a molecular weight of the order of 10^6. Its intrinsic viscosity $[\eta]$ equals 4.5. As will be seen, the data fall on straight lines for all the systems and we may extrapolate to $p = 0$, thus obtaining viscosity values characteristic of the polymer and *independent of the viscometer.*

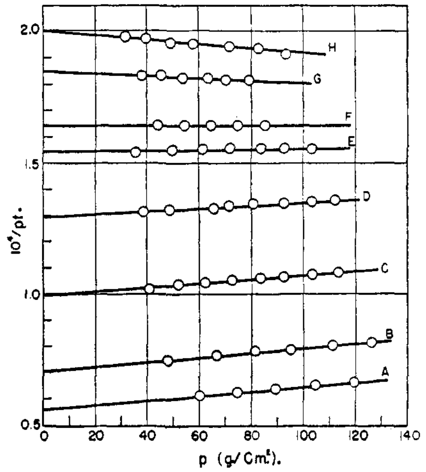

Fig. 4.—$(1/pt)$–p plots for a series of solutions of polyvinylpyridine in methanol. The concentration of polyvinylpyridine in g./100 ml. is as follows: (A) 0.3378, (B) 0.2637, (C) 0.1678, (D) 0.0979, (E) 0.0593, (F) 0.0452, (G) 0.0184, (H) 0.0000.

Still more important, we may now use Eq. (7) to obtain some information regarding the dependence of viscosity of polymers on rate of shear. Suppose we assume that Eq. (7) gives the dependence of apparent viscosity on pressure as far as drainage, end effect and kinetic energy corrections are concerned. Then any remaining dependence must be due to change of polymer viscosity increment with rate of shear. A test of this hypothesis is shown in Fig. 5. The dotted line is the ideal dependence of $\lambda\eta\rho$ on $(\rho/\eta)^2$ obtained by our calibration liquids. The circles show the dependence of the observed $S\eta\rho$ products for the polymer solutions of Fig. 4, where S is the slope from this figure. The difference between observed and ideal slopes will, by hypothesis, depend on change with pressure of the contribution of the solute to viscosity.

We now proceed to an analysis of this proposal. Let z be the reduced viscosity

$$(\eta - \eta_0)/\eta_0 = (\eta_r - 1) = \eta_{sp} = zc \qquad (12)$$

where η is solution viscosity at pressure p and concentration c, η_0 is solvent viscosity, η_r is relative viscosity and η_{sp} is specific viscosity. Let z_∞ represent the reduced viscosity at concentration c at zero rate of shear (zero pressure or infinite time). To avoid double subscripts, let j be the limit approached by the relative viscosity at zero rate of shear

$$j = \lim\,(\eta_r)_{p=0} = \eta_\infty/\eta_0 \qquad (13)$$

so that $j - 1 = z_\infty c$. Let η_∞ be the solution viscosity at the same limit. Now the contribution of the polymer to solution viscosity will be expected to change with changing velocity gradient, which

---

(8) H. Mark, *J. Appl. Phys.*, **12**, 41 (1941).

(9) R. M. Fuoss and U. P. Strauss, *Ann. N. Y. Acad. Sci.*, **51**, 836 (1949).

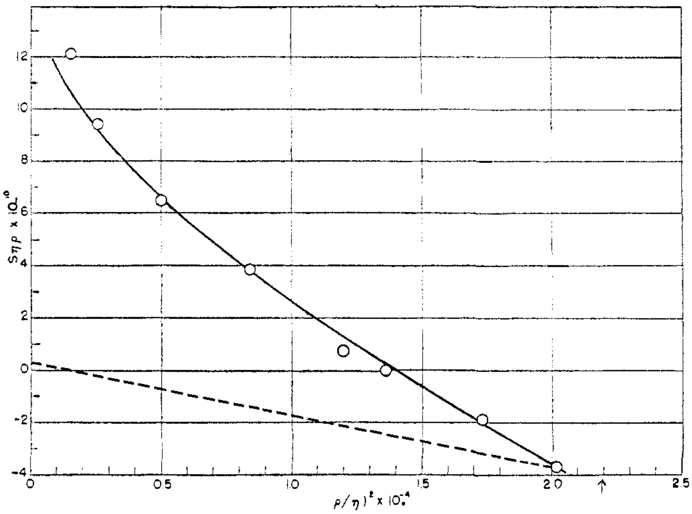

Fig. 5.—The dependence of the observed $S\eta\rho$ products on $(\rho/\eta)^2$ for the polymer solutions of Fig. 4 where S is the slope from this figure. The dotted line is the ideal dependence of $\lambda\eta\rho$ on $(\eta/\rho)^2$, *i.e.*, as far as drainage and kinetic energy corrections are concerned.

is, in turn, proportional to driving pressure. High rates of shear could both elongate the polymer coil and orient the ellipsoid hydrodynamically equivalent to the coil, which would tend to decrease viscosity; we, therefore, make the assumption that in first approximation

$$z = z(p) = z_\infty\,(1 - kp) \qquad (14)$$

where k is an arbitrary constant. From (12)

$$\eta = \eta_0\,(1 + zc)$$

Substituting (14) into the above expression, and using the abbreviations defined in the preceding paragraph, we find

$$\eta = \eta_\infty\,(1 - [j - 1]kp/j) \qquad (15)$$

Approximating $(1 - x)^{-1}$ as $(1 + x)$ in the equation for reciprocal viscosity, we obtain

$$\begin{aligned} 1/pt &= A_0/\eta - \lambda p \\ &= A_0/\eta_\infty - \lambda p + (A_0qk/\eta_0)p \qquad (16) \end{aligned}$$

where

$$q = (j - 1)/j^2 \qquad (17)$$

Eq. (16) is of the form

$$1/pt = A_0\,/\,\eta_\infty + (\kappa - \lambda)p \qquad (18)$$

where $\kappa = A_0qk/\eta_0$.

In other words, a polymer solution which is non-Newtonian will give in first approximation a linear $(1/pt)$–p plot with a slope dependent on concentration and molecular weight. The test of our assumption is to see whether the dependence of the slopes of Fig. 4 on concentration is given by Eq. (19); $q = q(C)$ by definition. The experimental values of κ are obtained by correcting the observed slopes S for drainage, end effects and kinetic energy according to Eq. (7). These corrections are read off the dotted line of Fig. 5. We then plot the values of κ against Aq/η_0 where experimental extrapolated values of j (*cf.* Eq. (13)) were used to compute q by means of Eq. (17). The points of Fig. 6 lie on a straight line through the origin and from the slope we find for the shear coefficient $k = 1.67 \times 10^{-3}$. For a polystyrene with molecular weight 670,000 and intrinsic viscosity 2.27 in toluene, $k = 0.36 \times 10^{-3}$. For the latter material, measurement of viscosity in an Ostwald viscometer, where the average driving pressure is about 10 g./sq. cm., would give an apparent viscosity which was 0.36% too low (if shear dependence of solute viscosity were the only cause of apparent variation of viscosity with pressure).

We may now reverse the procedure, having a numerical value for k, and compute theoretical $Sp\eta$ values for the systems of Fig. 4. The solid curve of Fig. 5 is computed on the basis of a *single* arbitrary constant k. The curve reproduces the observed values well within the experimental error of determining slopes from point-wise data.

As implied above, the slopes depend both on concentration and on molecular weight, because

$$z_\infty = [\eta] + k'[\eta]^2c \qquad (20)$$

and

$$[\eta] = KM^\alpha \qquad (21)$$

By extrapolating $(1/pt)$–p plots to zero pressure, we obtain reduced viscosities which are characteristic of the polymer molecule at rest. It should be emphasized that these are the values which should be extrapolated to zero concentration in order to obtain a true intrinsic viscosity which will be independent of the conditions of the viscosity measurements.

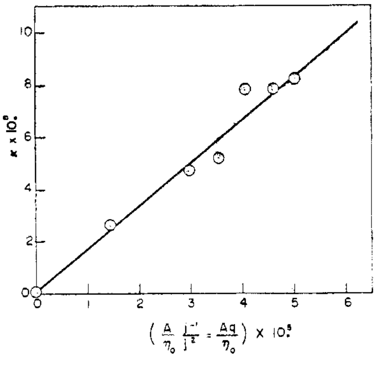

Fig. 6.—Experimental test of Eq. (19): data obtained from Fig. 4.

The shear constant k of Eq. (14) is, of course, an apparatus constant, because a given pressure produces a smaller velocity gradient in a smaller capillary for given V, l and η, since the flow time is increased (Table I of Ref. 9). If we combine Kroepelin's formula[10] for the average velocity gradient β in a capillary

$$\beta = 8V/3\pi R^3 \qquad (22)$$

with Eq. (1), we have, to an approximation accurate enough for a correction term

$$p = 3l\eta\beta/gr \qquad (23)$$

and Eq. (14) becomes

$$z = z_\infty(1 - 3\,kl\eta\beta/gr) = z_\infty(1 - s\beta) \qquad (24)$$

---

(10) H. Kroepelin, *Kolloid Z.*, **47**, 294 (1929).

where the shear constant s, defined as change of reduced viscosity with velocity gradient, is seen to be

$$s = (3l\eta/gr)k \tag{25}$$

Summary

1. The Wilberforce equation, which includes kinetic energy and end effect corrections for capillary viscometers, can be rearranged to an equation in which apparent fluidity is linear in driving pressure. An additional term, also linear in pressure, is produced by drainage errors. A method is described for the experimental evaluation of these corrections.

2. Polystyrene and polyvinylpyridine solutions exhibit a fluidity which varies linearly with pressure, after the above corrections have been made. This residual variation is ascribed to a distortion and/or orientation of the polymer molecule. Analysis of the data permits description of the shear dependence in terms of a single arbitrary constant k, the shear constant. At a pressure p, the intrinsic viscosity of a polymer is

$$[\eta]_\infty(1 - kp)$$

SCHENECTADY, NEW YORK RECEIVED MAY 9, 1950

[CONTRIBUTION FROM THE STERLING CHEMISTRY LABORATORY OF YALE UNIVERSITY]

Bolaform Electrolytes. I. Di-(β-trimethylammonium Ethyl) Succinate Dibromide and Related Compounds[1]

BY RAYMOND M. FUOSS AND DAVID EDELSON[2]

Introduction

We have been investigating the properties of polyelectrolytes[3] of the chain type and found it desirable to synthesize multivalent electrolytes of the same general structure, but of much lower molecular weight. For example, conductance data on the methyl bromide addition compound of the polyester obtained by condensing succinic anhydride and methyldiethanolamine[4] needed for their interpretation the limiting conductance of the monomer unit. Two general types of fundamental units could be considered, which may be represented schematically as

$$(\ldots\ldots+\ldots\ldots) \tag{1}$$

and

$$(+)\ldots\ldots\ldots\ldots(+) \tag{2}$$

In (1), we have a charged group at the center of a chain of atoms; in (2) we have a chain of atoms connecting two charged atoms. An example is shown in Fig. 1, which is a photograph of the Hirschfelder model of the di-(β-trimethylammonium-ethyl) sebacate ion. For the latter type, we propose the name[5] "bolaform" electrolytes; by extension of the meaning, we shall use the term to designate multivalent electrolytes of *low* molecular weight, *e.g.*, structures such as

$$(+)\ldots\ldots\ldots(+)\ldots\ldots\ldots(+) \tag{3}$$

and

$$(+)\ldots\ldots\begin{cases}\ldots\ldots\ldots(+)\\ \ldots\ldots\ldots(+)\end{cases} \tag{4}$$

In addition to their bearing on the polyelectrolyte problem, bolaform electrolytes show promise of being useful in understanding the behavior of multivalent simple ions. The calcium ion, for example, may be considered in an approximate sort of way as the limit of structure (2) as the chain of connecting ions shrinks to zero, and the lanthanum ion as the corresponding limit of structures (3) and (4). In other words, we hope to arrive at a better understanding of some of the peculiarities of multivalent ions by studying the properties of bolaform electrolytes and extrapolating to zero chain length.

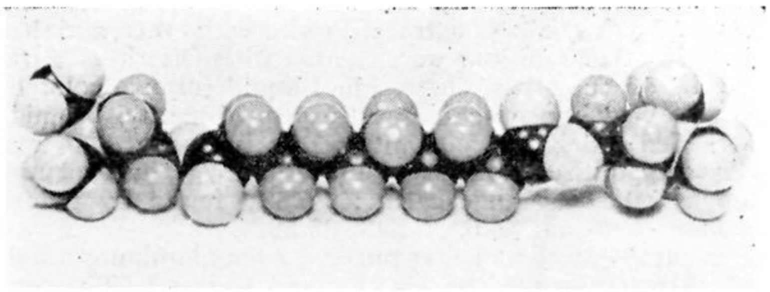

Fig. 1.—Hirschfelder model of di-(β-trimethylammonium-ethyl) sebacate ion.

In this paper, we present conductance data on two salts (I and II) of structure (1) and on one bolaform electrolyte (III) of structure (2). Data on other bolaform electrolytes[6] will be presented soon. These salts have the structures

$$[\mathrm{HO(CH_2)_2{\cdot}N^+Me_2(CH_2)_2OH}]\mathrm{Br}' \tag{I}$$

$$[\mathrm{CH_3CO_2(CH_2)_2N^+Me_2(CH_2)_2CO_2CH_3}]\mathrm{Br}' \tag{II}$$

$$\mathrm{Br}'[\mathrm{Me_3N^+(CH_2)_2CO_2(CH_2)_2CO_2(CH_2)_2N^+Me_3}]\mathrm{Br}' \tag{III}$$

Salts I and II behave like typical 1–1 electrolytes with large cations, while Salt III exhibits a behavior resembling that of 2–1 electrolytes. An analysis of the conductance curves of Salt III in methanol, in ethanol and in a mixture of these solvents shows that one anion is essentially free while the other is in association equilibrium[7] with the singly charged aggregate (−) (+).....(+).

---

[1] Office of Naval Research, Project NR 054-002; Paper No. 26.

[2] Results herewith presented were abstracted from a thesis presented by David Edelson to the Graduate School of Yale University, June, 1949, in partial fulfillment of the requirements for the Degree of Doctor of Philosophy in Chemistry.

[3] R. M. Fuoss, *Science*, **108**, 545 (1948).

[4] R. M. Fuoss and D. Edelson, *J. Polymer Sci.*, **5**, S33 (1950).

[5] "bola, a kind of missile weapon consisting of balls of iron, stone, etc., attached to the ends of a thong or cord ...... A third ball is sometimes attached to a cord nearly half as long as the main cord and at a point bisecting it." "Webster's New International Dictionary," Second Edition, Merriam Co., Springfield, Mass., 1938, p. 303.

[6] Victor F. Chu, Thesis, Yale University, 1950.

[7] R. M. Fuoss, *Chem. Revs.*, **17**, 27 (1935).